Materials Science & Engineering A 871 (2023) 144872

Contents lists available at ScienceDirect

Materials Science & Engineering A

journal homepage: www.elsevier.com/locate/msea

Temperature-dependent mechanical behavior of aluminum AM structures generated via multi-layer friction surfacing

Zina Kallien [a,*], Arne Roos [a], Christian Knothe-Horstmann [a], Benjamin Klusemann [a,b]

[a] Helmholtz-Zentrum Hereon, Institute of Materials Mechanics, Max–Planck-Straße 1, 21502 Geesthacht, Germany
[b] Leuphana University Lüneburg, Institute for Production Technology and Systems, Universitätsallee 1, 21335 Lüneburg, Germany

ARTICLE INFO

Dataset link: http://dx.doi.org/10.5281/zenodo.7615507

Keywords:
Friction surfacing
Additive manufacturing
Tensile strength
Temperature
Aluminum alloys
Solid state layer deposition

ABSTRACT

Multi-layer friction surfacing (MLFS) is a solid state layer deposition technology for metals. In order to make use of the potential of MLFS as technology for additive manufacturing, the material properties of MLFS built structures have to be investigated and understood in detail. This study presents a comprehensive analysis of the mechanical properties of MLFS deposited material from micro-flat tensile testing (MFTT) at elevated temperatures. The specimens obtained from the fine-grained MLFS structures show a slightly higher tensile strength at room temperature but lower tensile strength at testing temperatures of 300 °C and above compared to the stud base material. No significant gradient along the MLFS structure could be observed in terms of mechanical properties. The analyses of fracture surfaces and microstructure of tested MFTT specimens provide insights to deformation mechanism of MLFS deposited and consumable stud material. Especially at high testing temperatures of 500 °C, MLFS deposited structure shows abnormal grain growth which results in the observed tensile behavior.

1. Introduction

Additive manufacturing (AM) technologies are in high demand because they meet the requirements for lightweight and purpose-designed components. Commonly used fusion-based AM techniques such as direct energy deposition are powder- and wire-based technologies where a consumable material is molten and welded to a final structure [1]. However, fusion-based AM technologies bring also some challenges, e.g. pore formation or evaporation of alloying elements due to material melting and solidification or immense re-heating of the structure [2]. These issues are far reduced when solid state technologies are applied. For instance, the layer-by-layer generation of a structure can be achieved via a solid state layer deposition (SSLD) process, without melting the material. In this regard, the friction surfacing (FS) process variant of depositing multiple FS layers on top of each other is also known as multi-layer friction surfacing (MLFS) [3], where the heat input through re-heating of the structure is far reduced compared to conventional fusion-based AM technologies. FS was developed as coating technology for metallic materials, where the maximum temperatures of approximately 80 % of the material's melting temperature are reached during deposition, resulting in lower heat inputs and reduced heat affected zones compared to fusion-based processes [4].

Each MLFS layer deposition follows the principle of single layer FS. The deposition process is initiated by positioning a rotating consumable stud above a substrate material. When an axial force is applied, the rotating stud is pressed onto the substrate and friction leads to heat generation at the materials' interface. Due to the frictional heat, the tip of the stud deforms and plasticizes. Relative translational movement between stud and substrate is initiated at a defined travel speed and a layer of the plasticized consumable stud material is deposited on the substrate. During the process, the consumable material is subjected to severe plastic deformation and process heat, changing the microstructure of substrate and consumable material [5]. Essentially, the consumable material experiences a strong grain refinement enabled by dynamic recrystallization during deposition [6].

Being a discontinuous process, the dimension of a single deposited FS layer is limited by the dimension of the consumable stud used. Since deposited layers have some unbonded regions outside the main bonding area [7], further post-processing, e.g. machining, might be necessary. In order to overcome limitations in thickness and width of the deposited structure, FS process variants were developed: (i) MLFS, where multiple layers are deposited on top of each other; (ii) multi-track friction surfacing (MTFS), where multiple layers adjacent to and overlapping each other are deposited, see e.g. Soujon et al. [8]. For both FS process variants, the available studies are rare. Tokisue and coworkers [9,10] performed the deposition of a second layer next to the first one. The authors concluded that the tensile strength is

* Corresponding author.
E-mail address: zina.kallien@hereon.de (Z. Kallien).

https://doi.org/10.1016/j.msea.2023.144872
Received 20 December 2022; Received in revised form 14 February 2023; Accepted 2 March 2023
Available online 5 March 2023

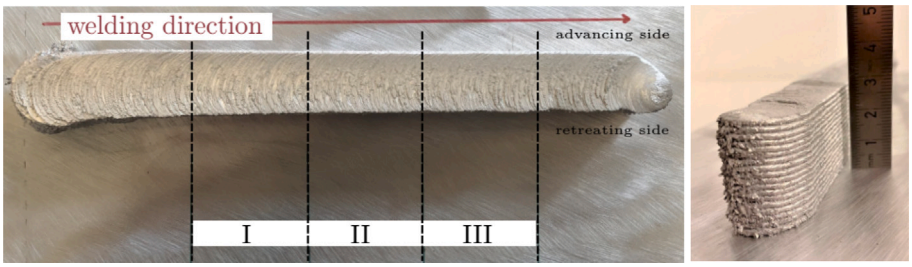

Fig. 1. MLFS structure for extraction of micro-flat tensile specimens. The tensile specimens were extracted from three parts of the weld: beginning (I), center (II) and end (III).

higher for the FS material in multiple layers compared to a single layer. Regarding MLFS, Galvis et al. [11] investigated the interfaces between substrate and coating as well as between two coating layers, which were deposited on top of each other. One finding was that the roughness of the first layer improves mechanical anchoring at the interface of first to second layer. MLFS structures consisting of three layers were also proven feasible for aluminum on steel [12] and aluminum on aluminum [13]. Shen et al. [14] showed FS in terms of MLFS being a highly repeatable process, creating sound bondings between each layer and a throughout homogeneous microstructure for six deposited FS layers. Rath et al. [15] performed micro-flat tensile testing for AA5083-H112 built on a AA2050-T84 substrate and investigated possible trends along MLFS deposit length as well as directional dependencies in terms of mechanical properties, where no significant anisotropy of the mechanical properties was observed.

The possibility to deposit multiple layers on top and adjacent to each other, i.e. a combination of MLFS and MTFS, was shown to be feasible for steel [16] and aluminum [8], which proves the potential of the FS process principle for AM applications. In order to fully exploit its potential, a fundamental understanding of the properties in the generated structures and the quality of the deposited material has to be achieved. With regard to further processing of FS-deposited material, possible future applications as well as modeling purposes, the mechanical behavior of the deposited material not only at room temperature but also at higher temperatures is of fundamental interest.

In this regard, this study presents a systematic and detailed characterization of tensile properties of MLFS deposited material at elevated temperatures. For the investigation AA5083-H112 consumable stud material is deposited onto AA2050-T84 substrate, i.e. similar material combination as used by Rath et al. [15]. The choice of a non-preciptation-hardenable Al–Mg alloy is based on the objective to investigate the fundamental effects of MLFS deposited material at elevated temperatures in depth at firstm without considering additional effects such as precipitates. The knowledge gained will be useful to assess the characteristic performance of MLFS deposited material also in comparison to conventional fusion-based AM technologies.

2. Materials and methods

A special purpose friction welding system (RAS, Henry Loitz Robotics, Germany) was used to perform the FS experiments of this study. The machine allows maximum axial forces up to 60 kN, maximum rotational speeds of 6000 rpm and a spindle torque up to 200 N m. The aluminum alloys used for the present study are AA5083-H112 for consumable studs (20 mm diameter, 125 mm length) and AA2050-T84 for the substrate (300 mm length, 130 mm width, 12.5 mm thickness). An 18-layer MLFS stack was build on the substrate, using the same process parameters as in previous studies for single layer FS [17] and MLFS [3,15], i.e. 8 kN axial force, 1200 rpm rotational speed and 6 mm/s travel speed, see Figs. 1 and 2a. All deposition processes were performed force-controlled.

The specimen extraction was done via electrical discharge machining (EDM), which allows a precise positioning of the specimens in the MLFS stack. To avoid any influence of possible unbonded edges, all samples were taken from the center of the build stacks, i.e. within the main bonding zone. Fig. 2(a) shows the schematic positioning and dimensions of the micro-flat tensile testing (MFTT) specimens in the MLFS structure, with MFTT specimen thickness of 0.5 mm. Nine MFTT specimens were tested at each testing temperature, where three samples were taken from each of the welding areas I, II and III along the MLFS stack, Fig. 1. The extruded rod raw material (25 mm diameter) was used to machine the consumable studs of 20 mm diameter via turning process as well as for extracting the base material (BM) MFTT specimens, Fig. 2(d).

The tensile tests at room temperature were performed at a 5 kN tensile machine (Zwick/Roell, Germany), where a 2.5 kN tensile machine (Zwick/Roell, Germany) was employed at elevated testing temperatures. The strain was always recorded using a laser extensometer (Fiedler Optoelektronik, Germany). The heating was performed using coils with controlled heating via a induction furnace (HTG-1500/0,5, Linn High Therm, Germany). The temperature in the clamping was controlled using a thermocouple. All tensile tests were performed position-controlled at 0.2 mm/min testing speed, resulting in quasi-static testing conditions. In addition to room temperature, testing temperatures were chosen to be 100 °C, 200 °C, 300 °C, 400 °C and 500 °C in order to get an overall assessment of the mechanical behavior.

The tested MFTT specimens were visually inspected using a light microscope (VHX-6000, Keyence, Germany). Further specimens of the MLFS stack were embedded and prepared according to common metallographic practices. The prepared specimens were investigated with light microscope before and after etching (Barker for 90 s at 25 V). The grain size of deposited material was analyzed in representative region of the MLFS stack using a scanning electron microscope (SEM) (Quanta 650, Thermo Fisher Scientific Inc., USA) equipped with an EDAX electron backscatter diffraction (EBSD) detector of the Velocity series (AMETEK Inc., USA). The EBSD data was acquired using 15 kV and a working distance of 16 mm at a step size of 0.2 µm. Additionally, the fracture surfaces of tested MFTT specimens were investigated using SEM, where images were acquired using secondary electrons (SE) mode at 15 kV.

3. Results and discussion

The individual layer deposition processes presented a homogeneous behavior indicated by a constant stud consumption, where the average stud consumption rate, i.e. the feed rate in axial force direction, was 1.72 ± 0.05 mm/s. The final stack showed a length of approximately 210 mm, a height of 27 mm and a width of 21 mm. The stud BM presents an average grain size of 25.1 µm, Fig. 2(c), where the MLFS deposited material shows a much finer and homogeneous grain size of 4.2 µm, Fig. 2(b), which matches findings by Shen et al. [14]. In addition to the homogeneous microstructure, MLFS deposited AA5083 material also presents a homogeneous hardness in the range of the consumable stud BM [3,15].

Rath et al. [15] found no significant directional dependency of the tensile properties of AA5083-H112 on AA2050-T84 via MLFS, therefore, all tensile specimens in this study were extracted normal to the

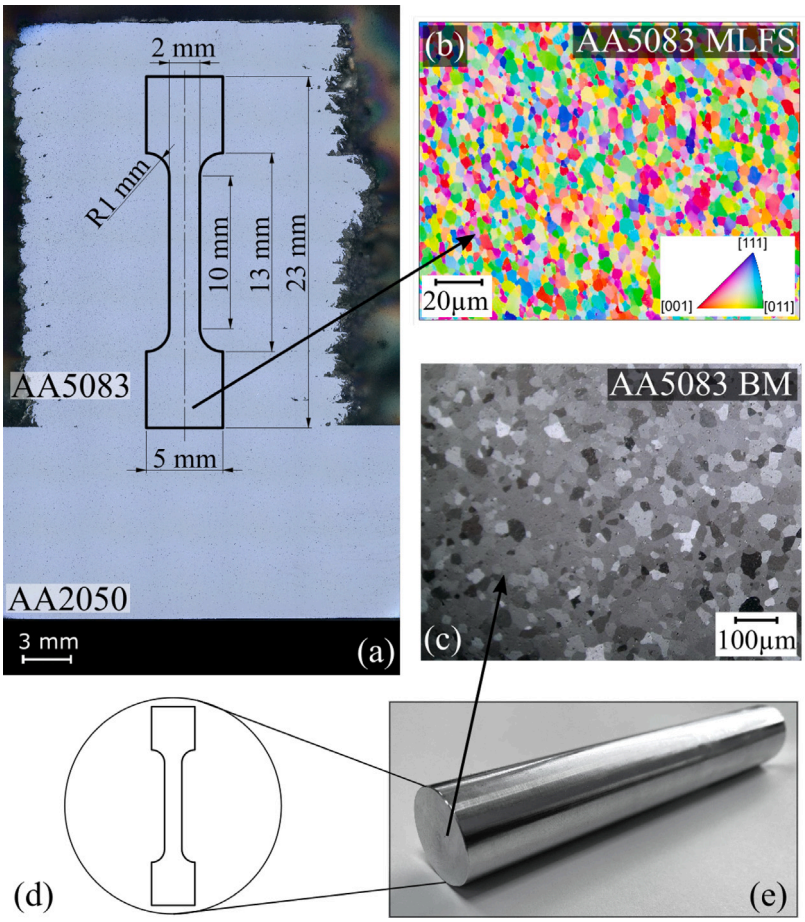

Fig. 2. Schematic of the positioning and dimensions of the MFTT specimens extracted from the built stack of 18 layers (a). Inverse pole figure map of MLFS deposited AA5083 material (b) and macrograph of BM etched with Barker solution for 90 s at 25 V (c). Position of MFTT specimen in raw BM (d) from which studs were machined (e).

substrate with similar orientation along the built structure, Fig. 2(a). In Fig. 3, the resulting stress–strain curves for exemplary MLFS and BM specimens are shown for different testing temperatures. As commonly for Al–Mg alloys, plastic deformation instabilities during tensile testing were observed at room temperature for both, MLFS and BM specimens, see Fig. 3(a). This behavior is known as Portevin-Le Châtelier (PLC) effect, leading to a serrated flow in the stress–strain curve [18]. The effect is the result of dislocations interactions with solute atoms through dynamic strain aging, which causes a spatial inhomogeneity of the plastic material flow [19].

In order to evaluate the mechanical properties of the MLFS deposited material at different temperatures in more depth, the mean values for yield ($R_{p0.2}$) and ultimate tensile strength (UTS) are extracted from the stress–strain data, see Fig. 4(b). However, since the tensile behavior of the MLFS material is observed to be constant along the MLFS structure, see Fig. 3(b), no further distinction is made between the different MLFS zones, i.e. MLFS I-III, see Appendix A for a detailed comparison.

Inherent to metallic materials, the strength decreases with increasing temperature. The comparison between MLFS and BM reveals that $R_{p0.2}$ and UTS are slightly higher for MLFS at room temperature, where this trend is reversed at higher testing temperatures. The UTS at room temperature is 25 MPa higher for the extracted MLFS material, Fig. 4(b), which corresponds to the findings of Rath et al. [15] as well as Silvério et al. [20]. The slightly increased strength of the MLFS material below 100 °C is most probably a result of the fine-grained microstructure of the MLFS structure, leading to the well-known Hall–Petch strengthening effect [21], whereas the grain boundaries hinder the movement of dislocations and lead to increased strength [22]. Overall, the results of the MFTT testing showed a very high reproducibility, i.e. low standard deviations in terms of the obtained strength values. In terms of elongation, no clear trend could be observed from the available data, see Appendix B. Therefore, the results in terms of elongation are not further discussed for brevity.

Exemplary tested MFTT specimens of BM and MLFS material, which were embedded, polished and etched, are shown in Fig. 5. The BM shows one distinct area at the gauge length were necking and failure occurred for all testing temperatures. For the MFTT specimens from the MLFS material, horizontal fracture can be observed at testing temperatures of 20 °C to 300 °C with little deformation of the material before fracture, i.e. without any pronounced necking. In contrast, at 400 °C and especially at 500 °C, the MLFS gauge length shows multiple areas where necking occurred.

To pursue the analysis on the mechanical behavior at different temperatures, the fracture surfaces of tested specimens at different temperatures were investigated via SEM. For the BM, Fig. 6, the fracture surfaces for tested samples from 20 °C to 300 °C show dimples, which are characteristic for a ductile behavior [23,24]. For increasing testing temperature, the BM fracture surfaces show deeper and larger dimples indicating the increased ductility of the material. The MLFS material's fracture surface for a specimen tested at room temperature also shows dimples but these are finer and more inhomogeneous compared to the BM, see Fig. 7. This corresponds to the findings of Jeong et al. [25], who reported the size of the dimples to decrease with decreasing grain size. The fracture surfaces of MLFS specimens tested at higher temperatures show a cleavage-like surface, Fig. 7. The fracture surface seems less rough than the BM at the same testing temperatures. This indicates a less ductile failure than the BM, confirming the observed behavior of MLFS compared to BM specimens below 400 °C. The SEM investigation

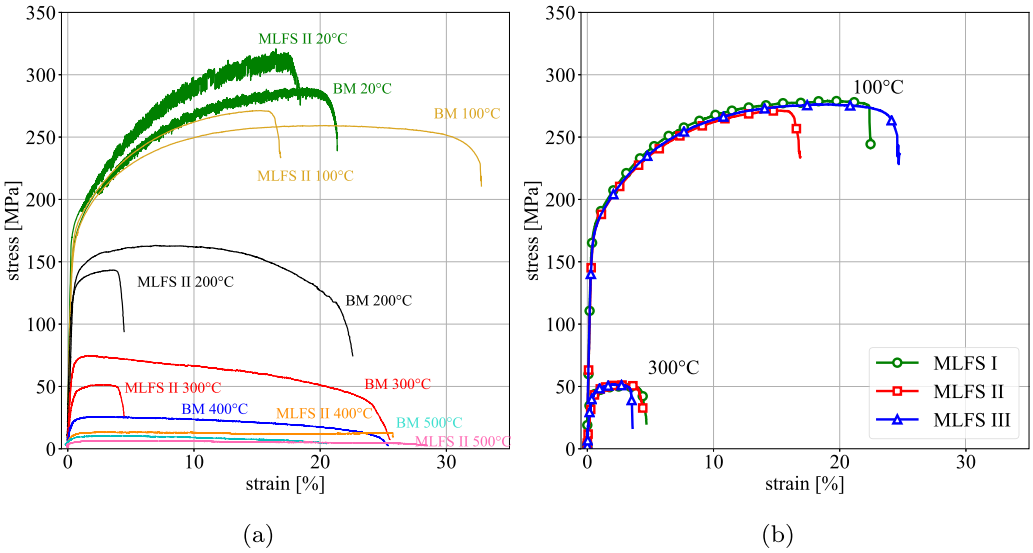

Fig. 3. Exemplary stress–strain curves for MLFS, taken at the center (MLFS II), and BM specimens at different testing temperatures (a) and for specimens along the MLFS stack (see Fig. 1) at 100 °C and 300 °C testing temperatures (b).

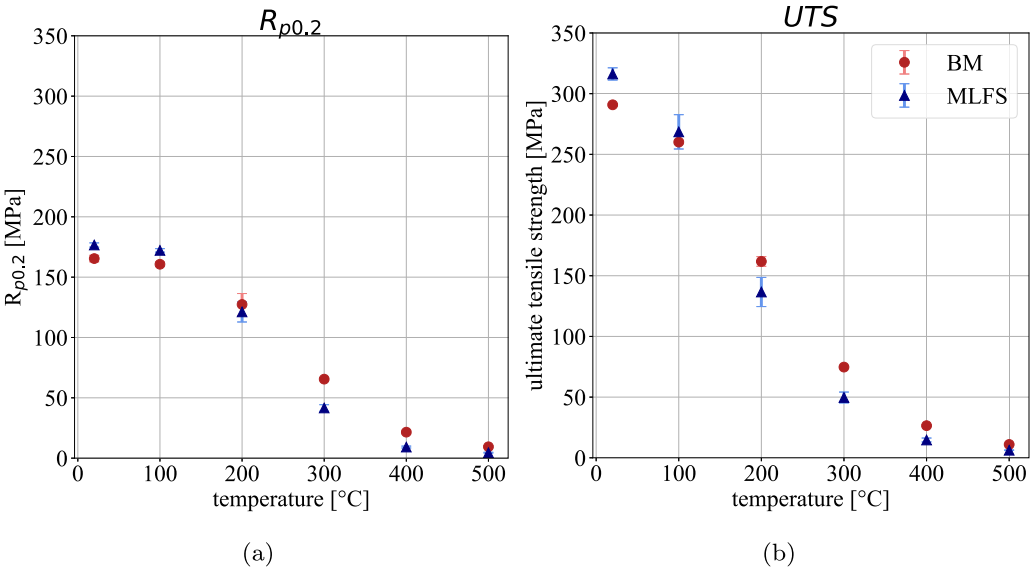

Fig. 4. Yield strength $R_{p0.2}$ (a) and ultimate tensile strength (b) for BM and MLFS deposited material at testing temperatures from 20 °C to 500 °C.

of MFTT specimens from MLFS material tested at 400 °C and 500 °C focused on the gauge length as it showed multiple sites where necking occurred.

High resolution images of the gauge width, where distinct necking occurred, were acquired using SEM for the 500 °C tested specimens, see Fig. 8, representing the material behavior at high testing temperatures. The BM samples showed one homogeneous necking area for all testing temperatures, Fig. 5(a), which is presented in detail in Fig. 8(a). In contrast, the MLFS specimens at high testing temperatures of 400 °C or 500 °C present multiple locations of necking along the gauge section, which can already be observed from the overview given in Fig. 5(b). The high resolution SEM macrograph of an exemplary MFTT specimen tested at 500 °C, Fig. 8(b), illustrates one of the edge-like structures that can be observed on the gauge length. The detailed analysis of the gauge length shows material transition zones, i.e. two different material behaviors can be observed alternately along the gauge length, where one region shows pronounced necking and the other is not significantly deformed. This might correlate with the interfaces between deposited layers. A deeper investigation of the microstructure is performed in the following in order to gain a more in-depth understanding of the observed phenomena.

The etched MFTT specimens reveal a homogeneous and stable microstructure for the BM, even up to 500 °C testing temperature, Fig. 5(a). A similar behavior is observed for the MLFS samples at first, however, massive grain growth is partially occurring in the initially fine-grained samples at 500 °C, Fig. 5(b). This leads to an inhomogeneous microstructure and consequently heterogeneous material behavior. In fact, necking occurred in the areas where the grains are fine, see also Fig. 9. The behavior might be attributed to grain boundary sliding [26], which is happening in the fine-grained part of the specimens where the ratio of grain boundaries is larger. Local necking occurred along the whole gauge section of the specimen and correlates well with the repeating inhomogeneous microstructure, Fig. 9. This resulting microstructure after grain growth might be related to the FS layer deposition process, due to small gradients of grain size within each individual deposited layer, which is typical for other AM processes as well [27]. This is in agreement with the observation by Rahmati et al. [28], where the grain size decreased from within the layer to the

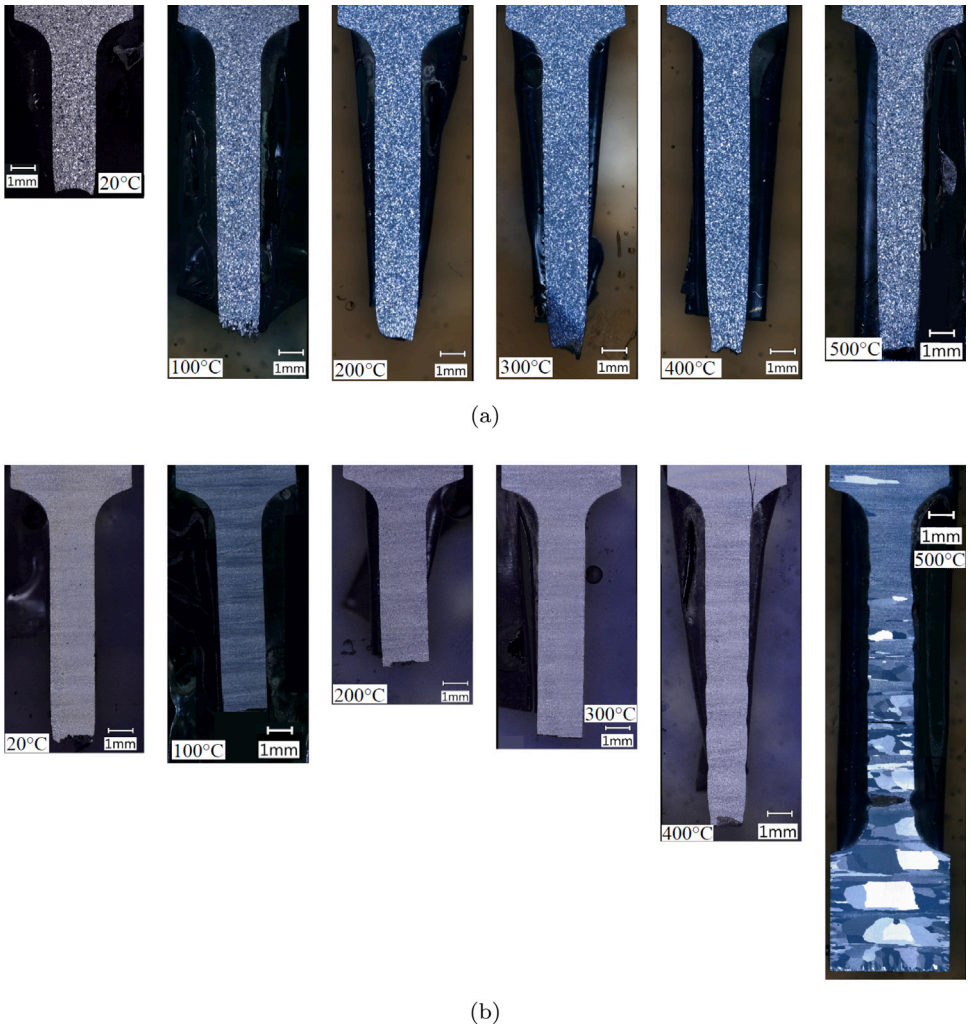

Fig. 5. Exemplary polished and etched MFTT specimens from BM (a) and MLFS material (b) tested between 20 °C and 500 °C.

layer-to-substrate interface for FS of AA2024 on AA1050. Therefore, the areas of fine grains, where necking occurred, seem to correspond to the layer interfaces. To support this hypothesis, simplified heat treatment experiments of the MLFS material were performed, where three layers were deposited and afterwards heated at different temperatures, see Appendix C. The results of these substitute experiments indicate significant grain growth already at 400 °C, which explains the change in the deformation behavior for the MLFS specimens observable from 300 °C to 400 °C. At 400 °C and above, local necking was detected at several locations along the gauge length, which can be explained by this phenomenon.

At room temperature, previous studies [8,15] did not observe a significant directional dependency for FS deposited aluminum alloys, where Rath et al. [15] showed that fracture sites could not be directly attributed to layer interfaces. However, grain growth within the layer at high testing temperatures, where grains seem to remain finer at the layers' interfaces, leading to grain boundary sliding and local necking along the gauge length. Therefore, a directional dependency of the MLFS material's tensile behavior cannot be excluded at such high temperatures due to the inhomogeneous microstructure formed.

4. Conclusion

The multi-layer friction surfacing process was applied to build an 18-layer stack, which showed reproducible deposition behavior of the non-precipitation-hardenable aluminum stud material and a homogeneous appearance for every layer. Micro-flat tensile testing specimens extracted from the MLFS stack at different locations along the deposition length were tested at room temperature as well as elevated temperatures. The main findings of this study can be summarized as follows:

- Specimens taken at the beginning, middle and end of the MLFS stack showed no significant differences in terms of tensile properties. The obtained strength values were highly reproducible at low standard deviations.
- At room temperature, the MLFS material showed slightly higher strength compared to the stud base material, which can be attributed to the Hall–Petch strengthening effect due to the fine-grained MLFS material.
- At elevated temperatures of 100 °C to 300 °C, MLFS material shows a slightly lower strength compared to the stud BM, where the fracture surfaces of the MLFS material also indicated a more brittle behavior.
- For testing temperatures of 400 °C and above, tensile specimens of MLFS material showed multiple areas of necking along the gauge length. The specimens tested at high temperatures partially experienced massive grain growth, with some areas where grains remained small. Necking occurred within regions of finer grains and can therefore attributed to grain boundary sliding.

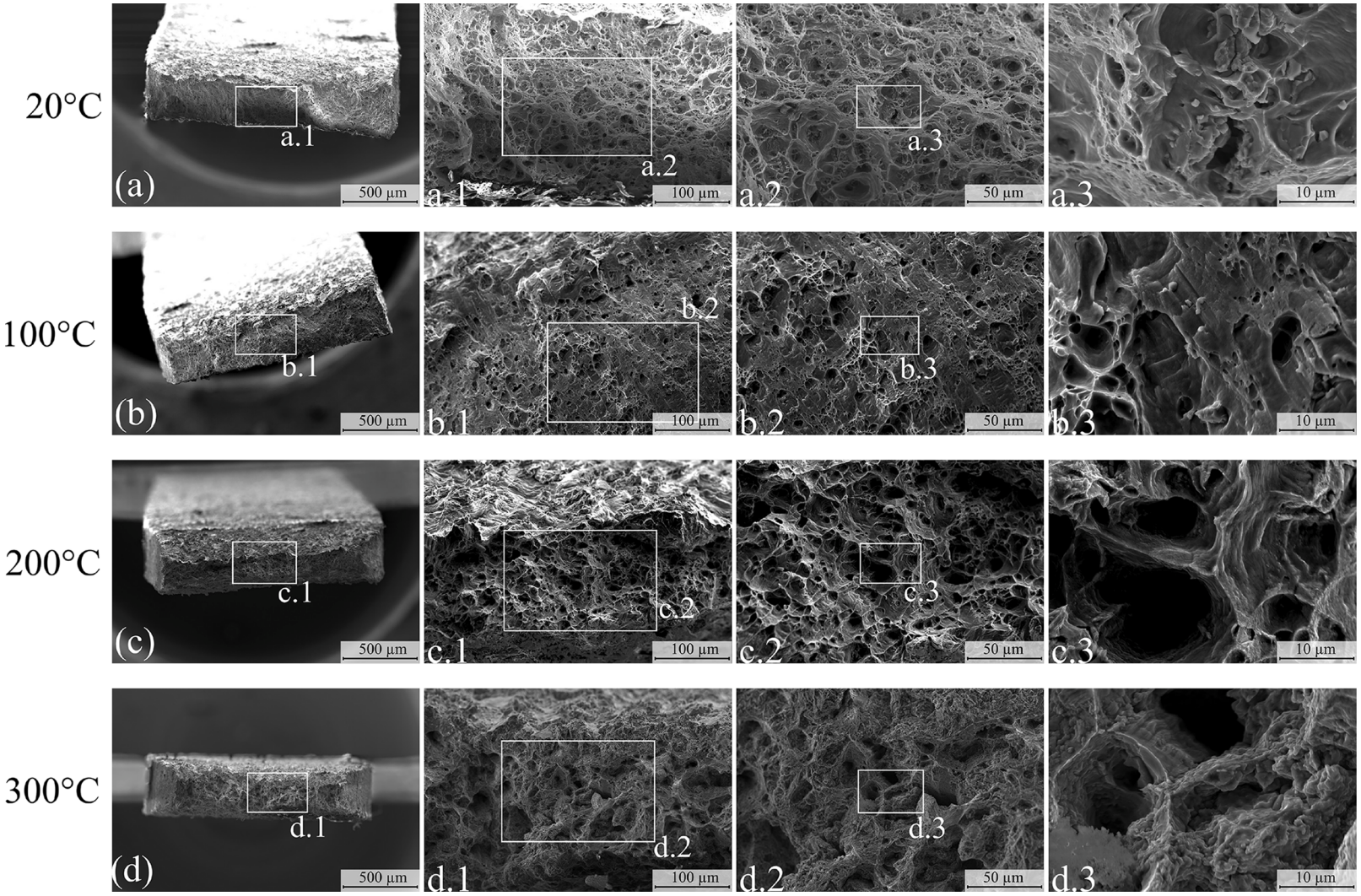

Fig. 6. Fracture surfaces of MFTT specimens of BM after tensile testing at different temperatures, i.e. 20 °C, 100°C, 200 °C and 300 °C.

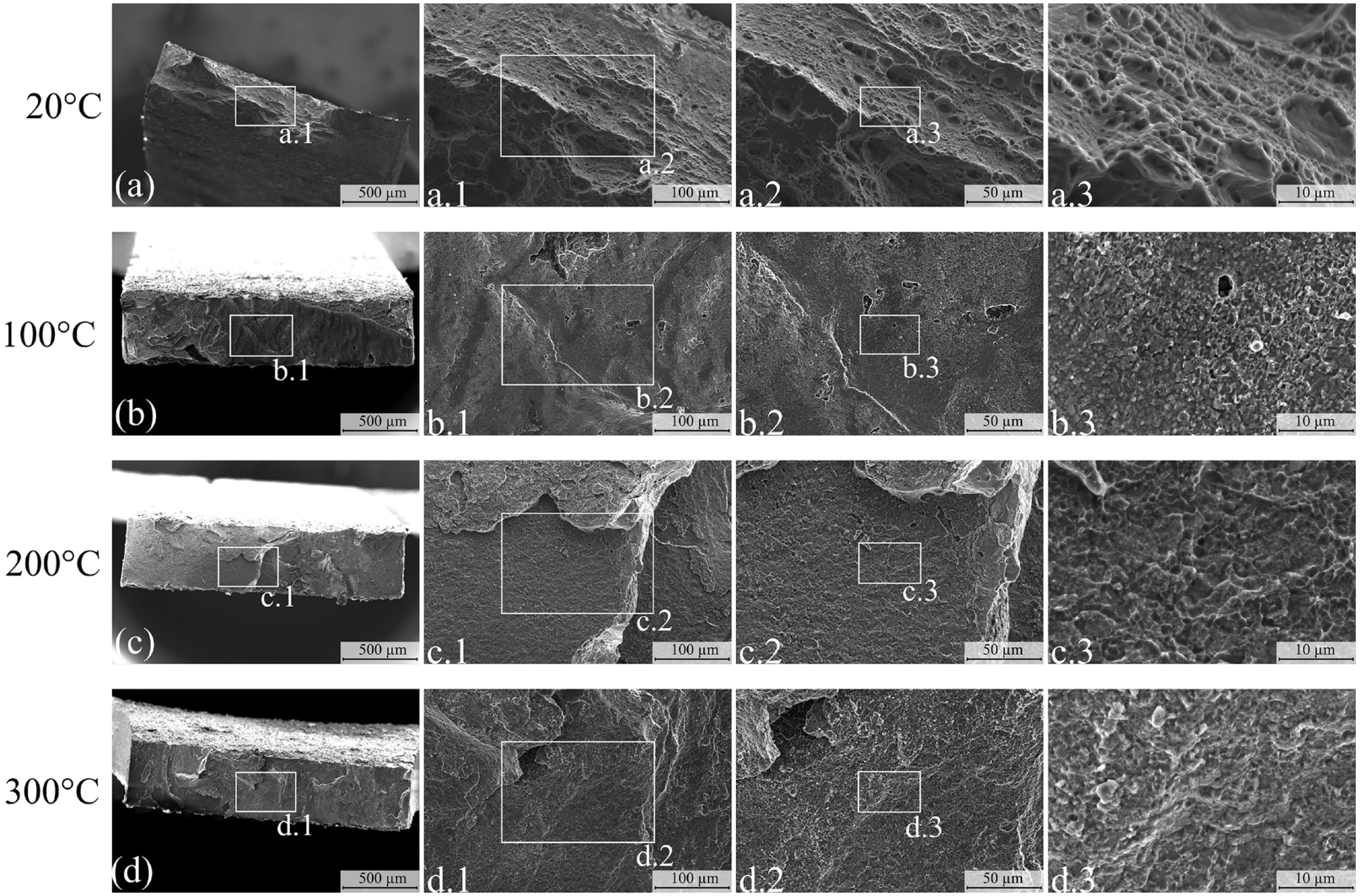

Fig. 7. Fracture surfaces of MFTT specimens of MLFS material after tensile testing at different temperatures, i.e. 20 °C, 100 °C, 200 °C and 300 °C.

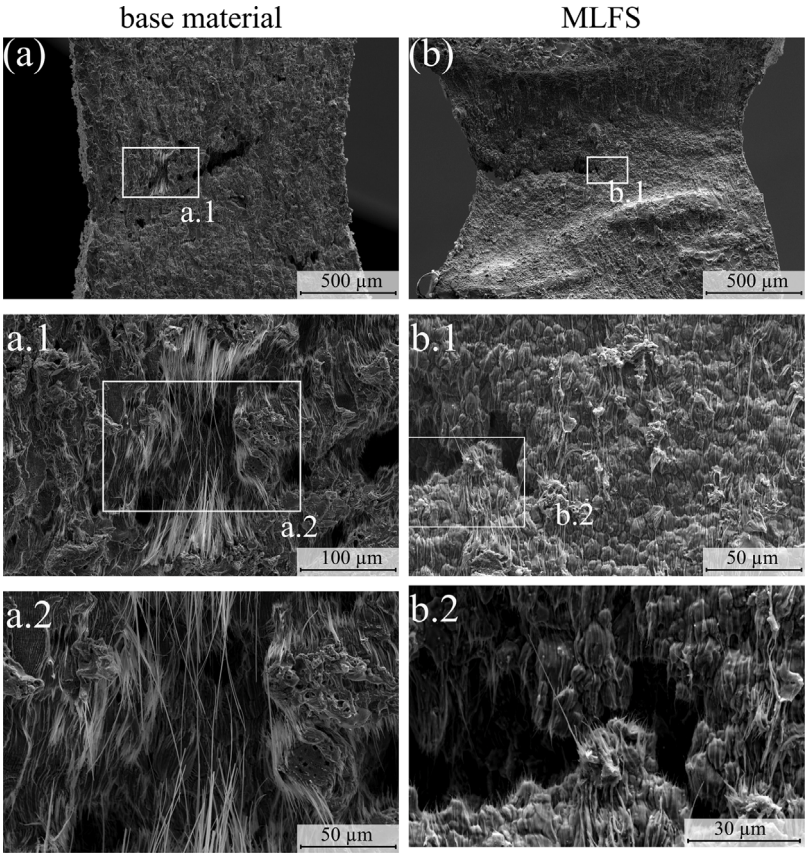

Fig. 8. Analysis of gauge section of MFTT specimens of BM (a) and MLFS (b) material tested at 500 °C.

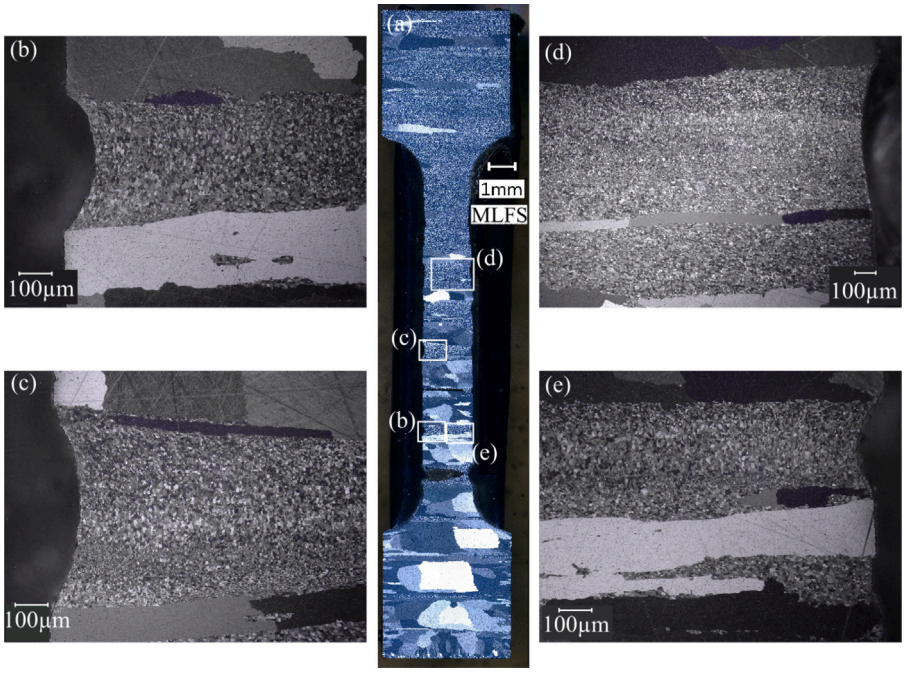

Fig. 9. MFTT specimen from MLFS structure tested at 500 °C, illustrating the local necking areas.

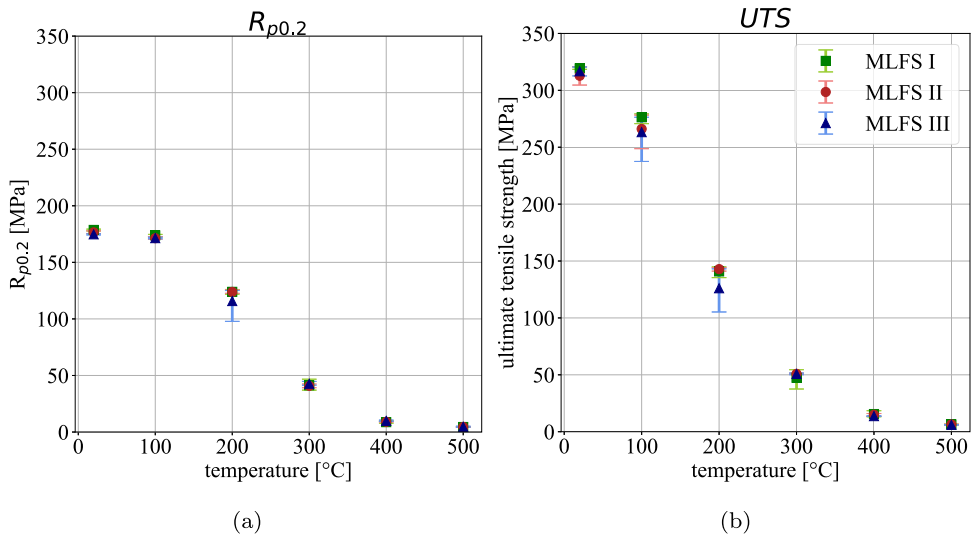

Fig. A.10. Yield stress (a) and ultimate tensile strength (b) for MLFS deposited material extracted from beginning (I), center (II) and end (III) along MLFS stack tested at temperatures from 20 °C room temperature to 500 °C.

In terms of MLFS, the layer by layer approach might also lead to further phenomena, which can have an effect on the resulting microstructure and the mechanical behavior, such as oxides at the layers' interfaces. Since FS generates new surfaces that could be highly reactive with the environment, the application of shielding gas concepts might be also a topic of future research [29], especially for MLFS.

CRediT authorship contribution statement

Zina Kallien: Conceptualization, Investigation, Data curation, Writing – original draft, Writing – review & editing, Visualization. **Arne Roos:** Writing – review & editing, Supervision. **Christian Knothe-Horstmann:** Writing – review & editing. **Benjamin Klusemann:** Conceptualization, Funding, Resources, Writing – review & editing, Supervision.

Declaration of competing interest

The authors declare that they have no known competing financial interests or personal relationships that could have appeared to influence the work reported in this paper.

Data availability

The obtained data of this research is online available at Zenodo (doi: http://dx.doi.org/10.5281/zenodo.7615507).

Acknowledgments

The authors would like to thank Mr. H. Tek from Helmholtz-Zentrum Hereon, Institute of Materials Mechanics, Laser Processing and Structural Assessment, for the support in conducting the tensile testing experiments.

Funding

This project has received funding from the European Research Council (ERC) under the European Unions Horizon 2020 research and innovation programme (grant agreement No 101001567).

Appendix A. Properties in different parts of MLFS structure

Fig. A.10[1] shows the results for $R_{p0.2}$ and UTS for each set of specimens in the individual areas along the deposition length, see Fig. 1. No significant difference can be observed for specimens extracted from start, center and end of the MLFS stack.

Appendix B. Elongation

Fig. B.11 shows the results for uniform elongation, A_g, and elongation at break, A. No clear trend could be observed from the available data, which might be related to unreliable detection of marks on the gauge length via laser extensometer especially at high testing temperatures.

Appendix C. Heating of deposited microstructure

In order to investigate the effect of temperature on the deposits' microstructure, an additional three-layer stack was welded using the same material combination (AA5083 over AA2050), similar process parameters (8 kN, 1200 rpm, 6 mm/s) and the same machine setup. After welding, the stack was cut into multiple samples. The samples were heated at the same temperatures that were used for tensile testing, i.e. 100 °C, 200 °C, 300 °C, 400 °C and 500 °C, for 20 min, which is approximately the duration of the tensile tests at elevated temperatures. The obtained cross sections of the samples are shown in Fig. C.12. Comparing the microstructures at room temperature and after 20 min heat treatment at 100 °C, 200 °C and 300 °C, no significant change in the deposits' microstructure can be observed, Fig. C.12(a)–(d). However, the cross section after 20 min heating at 400 °C reveals already some significantly coarser grains at the top of the stack as well as at the interfaces on the retreating side, Fig. C.12(e). The 500 °C heat treated sample shows a coarse grained microstructure for the whole stack, Fig. C.12(f). The largest grains can be observed in the center of the layers where the interfaces show finer grains. In comparison with the investigated BM, the MLFS material's microstructure seem to be less stable at elevated temperatures, leading to inhomogeneous grain growth along the building direction.

[1] Here mean value as well as minimum and maximum value are given in order to show the reproducibility of the obtained testing results.

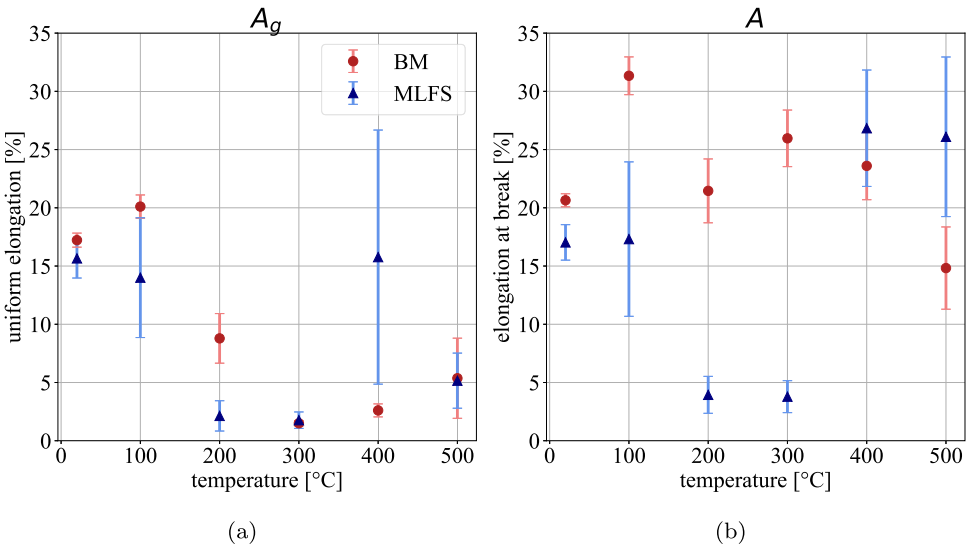

Fig. B.11. (a) uniform elongation, A_g, and (b) elongation at break, A, for micro-flat tensile testing of AA5083 consumable stud BM and MLFS deposited material.

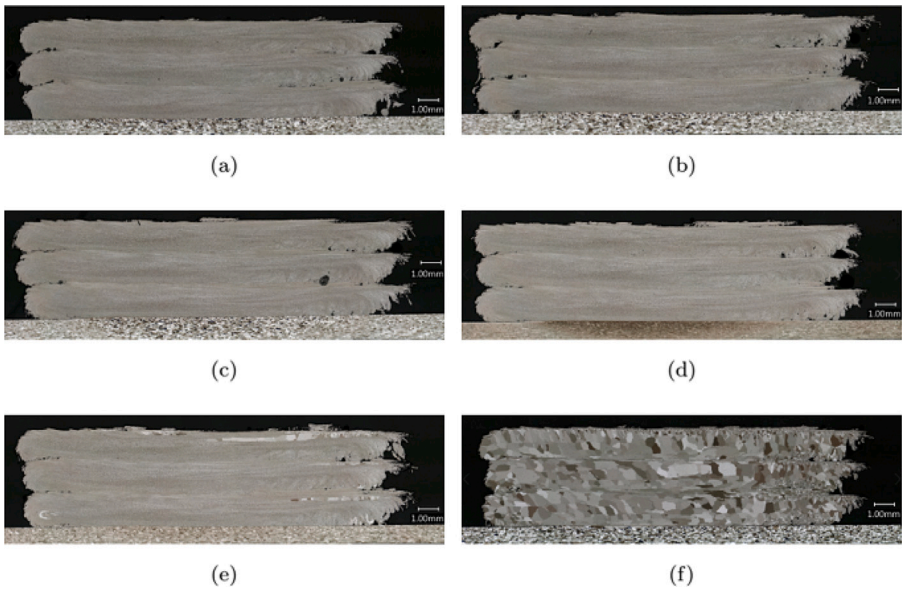

Fig. C.12. Macrographs of three-layer MLFS deposit after welding (a) and after 20 min heat treatment at temperatures of 100 °C (b), 200 °C (c), 300 °C (d), 400 °C (e) and 500 °C (f).

References

[1] D. Herzog, V. Seyda, E. Wycisk, C. Emmelmann, Additive manufacturing of metals, Acta Mater. 117 (2016) 371–392, http://dx.doi.org/10.1016/j.actamat.2016.07.019.

[2] O. Abdulhameed, A. Al-Ahmari, W. Ameen, S.H. Mian, Additive manufacturing: Challenges, trends, and applications, Adv. Mech. Eng. 11 (2), http://dx.doi.org/10.1177/1687814018822880.

[3] Z. Kallien, A. Roos, B. Klusemann, Experimental investigation of efficiency and deposit process temperature during multi-layer friction surfacing, Key Eng. Mater. 926 (2022) 187–193, http://dx.doi.org/10.4028/p-s43q63.

[4] J. Gandra, R.M. Miranda, P. Vilaça, Performance analysis of friction surfacing, J. Mater Process. Technol. 212 (8) (2012) 1676–1686, http://dx.doi.org/10.1016/j.jmatprotec.2012.03.013.

[5] H. Khalid Rafi, K. Balasubramaniam, G. Phanikumar, K. Prasad Rao, Thermal profiling using infrared thermography in friction surfacing, Metall. Mater. Trans. A 42 (11) (2011) 3425–3429, http://dx.doi.org/10.1007/s11661-011-0750-8.

[6] U. Suhuddin, S. Mironov, H. Krohn, M. Beyer, J.F. Dos Santos, Microstructural evolution during friction surfacing of dissimilar aluminum alloys, Metall. Mater. Trans. A 43 (13) (2012) 5224–5231, http://dx.doi.org/10.1007/s11661-012-1345-8.

[7] V.I. Vitanov, I.I. Voutchkov, Process parameters selection for friction surfacing applications using intelligent decision support, J. Mater Process. Technol. 159 (1) (2005) 27–32, http://dx.doi.org/10.1016/j.jmatprotec.2003.11.006.

[8] M. Soujon, Z. Kallien, A. Roos, B. Zeller-Plumhoff, B. Klusemann, Fundamental study of multi-track friction surfacing deposits for dissimilar aluminum alloys with application to additive manufacturing, Mater. Des. 219 (5) (2022) 110786, http://dx.doi.org/10.1016/j.matdes.2022.110786.

[9] H. Tokisue, K. Katoh, T. Asahina, Structures and Mechanical Properties of Multilayer Friction Surfaced Aluminum Alloys, Report of the Research Institute of Industrial Technology, Nihon University, (78).

[10] H. Tokisue, K. Katoh, T. Asahina, T. Ushiyama, Mechanical properties of 5052/2017 dissimilar aluminum alloys deposit by friction surfacing, Mater. Trans. 47 (3) (2006) 874–882.

[11] J.C. Galvis, P.H.F. Oliveira, J.d.P. Martins, A.L.M.d. Carvalho, Assessment of process parameters by friction surfacing on the double layer deposition, Mater. Res. 21 (3) (2018) 321.

[12] E.S. Abdelall, A.F. Al-Dwairi, S.M. Al-Raba'a, M. Eldakroury, Printing functional metallic 3d parts using a hybrid friction-surfacing additive manufacturing process, Prog. Addit. Manuf. 10 (3) (2021) 103, http://dx.doi.org/10.1007/s40964-021-00193-3.

[13] S. Krall, C. Baumann, H. Agiwal, F. Bleicher, F. Pfefferkorn, Investigation of multilayer coating of EN AW 6060 - T66 using friction surfacing, J. Mach. Eng. 22, http://dx.doi.org/10.36897/jme/147502.

[14] J. Shen, S. Hanke, A. Roos, J.F. Dos Santos, B. Klusemann, Fundamental study on additive manufacturing of aluminium alloys by friction surfacing layer deposition, AIP Conf. Proc. 2113 (2019) 10015.

[15] L. Rath, Z. Kallien, A. Roos, J.F. Dos Santos, B. Klusemann, Anisotropy and mechanical properties of dissimilar al additive manufactured structures generated by multi-layer friction surfacing, Int. J. Adv. Manuf. Technol. 117 (6) (2023) 371, http://dx.doi.org/10.1007/s00170-022-10685-3.

[16] J.J.S. Dilip, S. Babu, S.V. Rajan, K.H. Rafi, G.D. Janaki Ram, B.E. Stucker, Use of friction surfacing for additive manufacturing, Mater. Manuf. Process. 28 (2) (2013) 189–194, http://dx.doi.org/10.1080/10426914.2012.677912.

[17] Z. Kallien, L. Rath, A. Roos, B. Klusemann, Experimentally established correlation of friction surfacing process temperature and deposit geometry, Surf. Coat. Technol. 397 (2020) 126040, http://dx.doi.org/10.1016/j.surfcoat.2020.126040.

[18] S.P. Joshi, C. Eberl, B. Cao, K.T. Ramesh, K.J. Hemker, On the occurrence of Portevin–Le Châtelier instabilities in ultrafine-grained 5083 aluminum alloys, Exp. Mech. 49 (2) (2009) 207–218, http://dx.doi.org/10.1007/s11340-008-9208-3.

[19] M. Zaiser, P. Hähner, A unified description of strain-rate softening instabilities, Mater. Sci. Eng. A 238 (2) (1997) 399–406.

[20] S. Silvério, H. Krohn, V. Fitseva, N.G. d. Alcântara, J.F. d. Santos, Deposition of AA5083-h112 over AA2024-T3 by friction surfacing, Soldag. Insp. 23 (2) (2018) 225–234, http://dx.doi.org/10.1590/0104-9224/si2302.09.

[21] M. Ashjari, A. Mostafapour Asl, S. Rouhi, Experimental investigation on the effect of process environment on the mechanical properties of AA5083/Al2O3 nanocomposite fabricated via friction stir processing, Mater. Sci. Eng. A 645 (2015) 40–46, http://dx.doi.org/10.1016/j.msea.2015.07.093.

[22] R. Armstrong, 60 Years of hall-petch: past to present nano-scale connections, Mater. Trans. 55 (1) (2014) 2–12.

[23] E. Rincón, H. López, M. Cisneros, H. Mancha, M. Cisneros, Effect of temperature on the tensile properties of an as-cast aluminum alloy A319, Mater. Sci. Eng. A 452–453 (2007) 682–687, http://dx.doi.org/10.1016/j.msea.2006.11.029.

[24] R. Smerd, S. Winkler, C. Salisbury, M. Worswick, D. Lloyd, M. Finn, High strain rate tensile testing of automotive aluminum alloy sheet, Int. J. Impact Eng. 32 (1) (2005) 541–560, http://dx.doi.org/10.1016/j.ijimpeng.2005.04.013, fifth International Symposium on Impact Engineering.

[25] G. Jeong, J. Park, S. Nam, S.-E. Shin, J. Shin, D. Bae, H. Choi, The effect of grain size on the mechanical properties of aluminum, Arch. Metall. Mater. 60, http://dx.doi.org/10.1515/amm-2015-0115.

[26] T.G. Langdon, Grain boundary sliding revisited: Developments in sliding over four decades, J. Mater. Sci. 41 (3) (2006) 597–609, http://dx.doi.org/10.1007/s10853-006-6476-0.

[27] M. Frönd, V. Ventzke, F. Dorn, N. Kashaev, B. Klusemann, Microstructure by design: An approach of grain refinement and isotropy improvement in multi-layer wire-based laser metal deposition, Mater. Sci. Eng. A 772 (2020) 138635, http://dx.doi.org/10.1016/j.msea.2019.138635.

[28] Z. Rahmati, H. Jamshidi Aval, S. Nourouzi, R. Jamaati, Effect of friction surfacing parameters on microstructure and mechanical properties of solid-solutionized AA2024 aluminium alloy cladded on AA1050, Mater. Chem. Phys. 269 (2021) 124756, http://dx.doi.org/10.1016/j.matchemphys.2021.124756.

[29] J. Gandra, H. Krohn, R.M. Miranda, P. Vilaça, L. Quintino, J.F. Dos Santos, Friction surfacing—a review, J. Mater Process. Technol. 214 (5) (2014) 1062–1093, http://dx.doi.org/10.1016/j.jmatprotec.2013.12.008.